Atmos. Chem. Phys. Discuss., 9, 23141–23185, 2009
www.atmos-chem-phys-discuss.net/9/23141/2009/
© Author(s) 2009. This work is distributed under
the Creative Commons Attribution 3.0 License.

Atmospheric Chemistry and Physics Discussions

This discussion paper is/has been under review for the journal Atmospheric Chemistry and Physics (ACP). Please refer to the corresponding final paper in ACP if available.

Latitudinal gradient and interannual variation of PM_{10} concentration over eighty-six Chinese cities

W. J. Qu[1,2], R. Arimoto[3], X. Y. Zhang[2], Y. Q. Wang[2], L. F. Sheng[1], and G. Fu[1]

[1]Key Laboratory of Physical Oceanography, Ocean-Atmosphere Interaction and Climate Laboratory, Department of Marine Meteorology, College of Physical and Environmental Oceanography, Ocean University of China, 238 Songling Rd., Laoshan District, Qingdao 266100, China
[2]Key Laboratory of Atmospheric Chemistry, Centre for Atmosphere Watch and Services (CAWAS), Chinese Academy of Metrological Sciences, China Meteorological Administration, 46 Zhong-Guan-Cun S. Ave., Beijing 100081, China
[3]Carlsbad Environmental Monitoring and Research Center, New Mexico State University, Carlsbad, New Mexico, USA

Received: 5 September 2009 – Accepted: 19 October 2009 – Published: 2 November 2009

Correspondence to: W. J. Qu (quwj@ouc.edu.cn, quwj@163.com)

Published by Copernicus Publications on behalf of the European Geosciences Union.

Abstract

The spatial distribution of the aerosols over 86 major Chinese cities was constructed from 137 845 daily averaged PM_{10} (particles with diameter $\leq 10\mu m$) concentrations calculated from air pollution index (API) records spanning from summer 2000 to winter 2006. This dataset was based on days when PM_{10} was categorized as the principal pollutant, accounting for 91.6% of the total recorded days. The 83 cities in mid-eastern China (longitude 100° E to 130° E) were separated into three latitudinal zones with the Qinlin Mountain – the Huaihe River and the Yunnan-Guizhou Plateau – the Jiangnan Hill – the Wuyi Mountain as the boundaries. The spatial distribution of PM_{10} was complicated; the high-value spots in northern China (concentration ranged from 127.1 to 192.1 μgm^{-3}) included Urumchi, Lanzhou-Xining, Weinan-Xi'an, Taiyuan-Datong-Yangquan-Changzhi, Pingdingshan-Kaifeng, Beijing-Tianjin-Shijiazhuang, Jinan, and Shenyang-Anshan-Fushun; in the middle zone, the high PM_{10} spots (concentration within 119.1–146.6 μgm^{-3}) were Chongqing-Chengdu-Luzhou, Changsha-Wuhan, and Nanjing-Hangzhou; while in the southern zone, four cities (Qujing, Guiyang, Guangzhou and Shaoguan) showed higher PM_{10} concentration (>80μgm^{-3}). An overall latitudinal gradient was distinct; the median PM_{10} concentrations decreased from 108 μgm^{-3} for the 38 northern cities to 95 μgm^{-3} and 55 μgm^{-3} for the middle (26 cities) and southern (19 cities) zones, respectively. Linear regression between PM_{10} concentration and latitude of the cities also confirmed this gradient. PM_{10} concentration and the APIs exhibited similar seasonality with wintertime maxima and summertime minima, and the second highest values in spring. PM_{10} level showed a decreasing trend (–23.2μgm^{-3}) for the northern cities during 2000 to 2006. For the other two zones, the PM_{10} levels fluctuated, but showed unobvious change (–1.7μgm^{-3}) for the middle zone and increased slightly (+6.2μgm^{-3}) for the southern zone during the course.

ACPD

9, 23141–23185, 2009

1 Introduction

The atmospheric aerosol plays an important role in visibility impairment (Watson, 2002), and studies of potential aerosol effects on climate have become of increasing interest following the pioneering work of Twomey (1977) and Charlson et al. (1992). Concerns over adverse influences on human health (Pope et al., 1995) have added to scientific and public interest in aerosol particles.

Defining a representative aerosol distribution is essential for understanding the aerosols' effects on climate, especially over regional scales. However, it is challenging because the atmospheric aerosol shows greater spatial and temporal variations than most trace gases owing to the relatively short residence times of the particles and the heterogeneity of their sources (Kaufman et al., 2002). Aerosol distributions over the continent are generally patchy because of the diversity in emissions (especially ahthropogenic sources), unevenness in population density, and variations in terrain, which can influence the dispersion of air pollutants. In this context, there obviously exist gradients in aerosol concentrations, which potentially result in different regional climate effects. For example, data from an aircraft study over the Los Angeles Basin revealed horizontal gradients in aerosol concentrations that could result in variability of more than 50% within a 5×5km computational grid cell, a size commonly used in atmospheric models (Collins et al., 2000). Related studies over the tropical Indian Ocean indicated that the gradients in aerosols could lead to an inter-hemispheric difference in the solar heating (Rajeev and Ramanathan, 2001). Along these same lines, a gradient in the aerosol optical depth from the northern Arabian Sea to south of the Intertropical Convergence Zone (ITCZ) could lead to a gradient in the reduction of the noontime solar flux from as much as $-38 \mathrm{Wm}^{-2}$ in the Arabian Sea to as little as $-2 \mathrm{Wm}^{-2}$ south of the ITCZ, thus producing a strong north to south gradient in the climate forcing over the ocean (Meywerk and Ramanathan, 1999). Recent research has confirmed a strong latitudinal gradient in the total aerosol and black carbon (BC) over the Bay of Bengal with both decreasing rapidly from north to south (Nair et al., 2008). In addition

ACPD
9, 23141–23185, 2009

to these latitudinal aerosol gradient, a strong west-to-east gradient of BC has also been observed during research cruises along latitudes of 30° N and 35° N over the central Pacific Ocean from 1993 to 1996, and this effect was attributed to outflow from Asia (Kaneyasu and Murayama, 2000).

As for the health impacts of air pollution, the sources of air pollutants are mostly restricted to the earth's surface except for aircraft emissions in the upper troposphere (Highwood and Kinnersley, 2006); meanwhile approximately 47% of the global population lives and works in the generally most polluted urban areas. Investigations of surface air quality over urban areas and strategies for its improvement are therefore compelling.

China, a developing country with the world's largest population, has undergone rapid economic growth since economic reforms began in 1978. Along with urbanization and industrialization, China's economic growth has resulted in an increase in energy consumption, and this has brought with it the challenges of air pollution. Investigations of the spatial distribution and interannual variations in the atmospheric aerosol and air pollutants are necessary to understand the aerosol's regional climate effects and for the development and implementation of effective air pollution control strategies.

There have been numerous ground-based studies (measurement of the physical and chemical properties) of the aerosols in China, including those conducted at remote sites (Tang et al., 1999; Li et al., 2000; Qu et al., 2008), regionally representative rural sites (Xu et al., 2002; Wang et al., 2004a; Zhang et al., 2005) and urban sites in large and mega cities (Fang et al., 1999; Davis and Guo, 2000; He et al., 2001; Zhang et al., 2002; Cao et al., 2003; Ye et al., 2003; Ta et al., 2004; Duan et al., 2005; Wu et al., 2005; Zheng et al., 2005; Feng et al., 2006; Li et al., 2006, 2008; Meng et al., 2007; Chu et al., 2008). However, even taken together, these earlier studies do not provide a systematic picture of the spatial distribution of the aerosol across China. This is in part because of the limited and discontinuous coverage of most observations and also because of difficulties in inter-comparing results among research groups who use different sampling instruments and methods. As a result, there is limited information

ACPD
9, 23141–23185, 2009

on the spatial distribution of the surface aerosol across the country.

On the other hand, based on the radiation/optical measurement network and satellite observation, a lot of works have provided spatial distribution of aerosols over China as well (Luo et al., 2000, 2001; Li et al., 2003; Wang et al., 2008). However, the columnar aerosol optical depth (AOD) or aerosol optical thickness (AOT) derived from these optical observations is influenced by several factors including the vertical structure and height of the atmospheric mixing layer; therefore, the characteristic and variation of the AOD/AOT appear some difference from those of the surface aerosol, which will be discussed later (Sect. 3.7).

As an inhalable particulate pollutant, PM_{10} (particles with diameter $\leq 10\mu$m) is of primary concern for most Chinese cities, and PM_{10} is often reported as the principal pollutant (abbreviation as P_{prin} hereinafter) for the urban areas according to the environment monitoring system operated by the Environmental Protection Agency of China (EPA-China). In this paper we make use of 137 845 daily air pollution index (API) records for 86 major cities (Fig. 1, Table 1) to estimate the concentrations of PM_{10} over urban areas in China. The results are then used to study the spatial variability of PM_{10} and to evaluate its seasonal and interannual variations.

2 Data and methods

2.1 Air pollution index (API) data

The Chinese air pollution index (API) is a semi-quantitative measure for uniformly reporting air quality based on a group of atmospheric constituents that can affect human health. The API for each city, which is reported daily, converts the concentrations of the pollutants of interest into a dimensionless number from 0 to 500. To calculate the APIs, (1) five pollutants (PM_{10}, SO_2, NO_2, CO and O_3) are to be continuously measured at several monitoring stations in different districts or function districts (commercial, cultural, downtown, residential, traffic, industrial, etc.) of a city, also including

ACPD
9, 23141–23185, 2009

clean background station; (2) the daily average concentrations of these pollutants are then calculated according to the measurements made at all of the stations (however, CO and O_3 are reported as hourly mean); (3) a sub-pollution index (sPI) is calculated for each pollutant by linear interpolation of the average concentration of the specific pollutant between the grading limited values for each air quality classification listed in Table 2, and (4) the maximum sPI is reported as the API for the city and day. The API can thus reflect the averaged air quality in the entire city area (including the polluted districts and the clean areas). Air quality classifications corresponding to the APIs, air quality management recommendations, and pollutant concentrations are summarized in Table 2. Further information about the API may be found in Zhang et al. (2003) and Chu et al. (2008).

API records for 86 major Chinese cities (State Environmental Protection Agency, available at http://www.sepa.gov.cn/quality/air.php3) covering June 2000 to February 2007 were used in this study. Spatial coverage of data is concentrated in mid-eastern China (east of 100° E) (Fig. 1, Table 1). The data set comprises a total of 150 428 observations: the data for 41 cities spans ~7 years (June 2000 to February 2007), 6 cities cover ~6 years (June 2001 to February 2007), 37 cities ~3 years (June 2004 to February 2007), and 2 cities ~1 year (January 2006 to February 2007, Table 1).

2.2 PM_{10} data

For the days when PM_{10} was reported as P_{prin}, daily PM_{10} concentrations were derived from the APIs by using the following equation:

$$C = [(I - I_{low})/(I_{high} - I_{low})] \times (C_{high} - C_{low}) + C_{low}, \quad (1)$$

where C is the concentration of PM_{10}, I is API reported. I_{low} and I_{high} represent API grading limited value lower and larger than I, respectively; C_{high} and C_{low} denote the PM_{10} concentrations corresponding to I_{high} and I_{low} (Table 2), respectively. The method for calculating PM_{10} concentrations from APIs has been described in detail by Zhang et al. (2003). A total of 137 845 PM_{10} concentrations were calculated using this approach,

ACPD
9, 23141–23185, 2009

and this accounts for 91.6% of the APIs records. The other 8.1% and 0.3% of the APIs records correspond to days when SO_2 or NO_2 was reported as P_{prin}. Characteristics of the deduced PM_{10} concentrations are the main focus of this paper.

In China, PM_{10} concentration is generally measured by Tapered Element Oscillating Microbalance (TEOM)-based analyzer (model 1400a, Rupprecht & Patashnick, USA) at several stations in the major cities by the EPA-China environment monitoring system. The uncertainty of the daily PM_{10} measurement is typically less than 1% (Xia et al., 2006). However, for some cities and stations, β ray particulate monitor (model BAM-1020, Met One, USA) was used to monitor PM_{10} concentration. The principle of TEOM analyzer and β ray particulate monitor as well as their field application are summarized elsewhere (Bari et al., 2003; http://www.metone.com/documents/BAM-1020_6-08.pdf).

It is worth noting that for the days when PM_{10} was P_{prin} and the API was reported as 500, the PM_{10} mass loading actually could have exceeded the upper limit (600 $\mu g m^{-3}$) for the air quality classification of "high-level pollution". Such high paticulate loading can occur during severe dust storms in some northern cities. However, in this study, we dealt all the APIs records of 500 as the deduced PM_{10} concentrations equal to 600 $\mu g m^{-3}$. Moreover, there was no P_{prin} reported on days when the API was less than 50 (the air quality "clean"). Inspection and comparison of the sPIs of PM_{10}, SO_2 and NO_2 for several cities indicated that for these cases, PM_{10} pollution is mostly prominent with the highest sPIs; this comparison based on the daily sPI records we have collected for some cities. Therefore for the days when no P_{prin} reported, we assumed in this study that PM_{10} was P_{prin} that day and deduced PM_{10} concentration according to Eq. (1).

As the data quality (the validity of this PM_{10} data set) is of the foremost concern, a comparison was conducted between this study and the related previous works (please see supplementary material 1 http://www.atmos-chem-phys-discuss.net/9/23141/2009/acpd-9-23141-2009-supplement.zip). Note several unrepresentative works, which tried to depict the air pollution conditions with limited measurements during a rather long period, were not included in this comparison. PM_{10} values calculated from API in this study were generally comparable with the literatures reported aerosol

ACPD
9, 23141–23185, 2009

concentrations (supplementary material 1 http://www.atmos-chem-phys-discuss.net/9/23141/2009/acpd-9-23141-2009-supplement.zip), which used other measurement methods such as filter sampling/gravimetry in field observation experiments. Linear regression between the API deduced PM_{10} concentration and the literatures reported PM_{10} concentration (Fig. 2) yields a correlation coefficient of 0.84 ($p<0.0001$ significance), which validated the PM_{10} concentration derived from the API in this study. According to the linear regression analysis, the literatures reported PM_{10} concentration is about 1.1 times the API deduced PM_{10} concentration. Because of difference in site selection–clean background site also included in the monitoring stations designed to obtain API, it is plausible that the literatures reported aerosol concentrations, which mostly observed at residential, commercial or traffic sites, are generally higher than the API deduced PM_{10} values.

In addition, it is reported that the results of the TEOM-based analyzer, which is generally used in the EPA-China's air quality monitoring network, can be comparable with the results of other instruments if multiplied by a factor of 1.3 due to the measurement condition of TEOM (50°C) and volatility of the aerosols (King, 2000). Other researches (Okuda et al., 2004, 2008; Bi et al., 2007) also reported such kind of comparison, which got similar results and confirmed validity of the API data set. The monthly mean PM_{10} concentrations reported by EPA-China in Nanning city during 2006 were close to those from the atmospheric composition observation network under China Meteorological Administration, and they present the same variation trend (Mo et al., 2008). Moreover, the daily PM_{10} observation results in Qingdao (at Baguanshan site, 36°03′44″ N, 120°20′08″ E, on the campus of Ocean University of China) during May 2007 to March 2008 (unpublished data) were also strongly correlated with the local API derived daily PM_{10} concentrations ($r=0.77$, $p<0.0001$ significance, $n=131$), and the filter collecting/gravimetry measured PM_{10} concentration was about 1.3 times the API deduced PM_{10} concentration. Such comparison and analysis confirm the validity of the API deduced PM_{10} data used in this study.

CC BY

2.3 Grouping of the cities according to the APIs

A hierarchical clustering procedure based on Ward's method and squared Euclidean distance was used to determine the similarities between the APIs of the cities. In addition, the correlations between among the APIs (please see supplementary material 2 http://www.atmos-chem-phys-discuss.net/9/23141/2009/acpd-9-23141-2009-supplement.zip) and the geographical locations of these cities were also taken into account in the grouping procedure. For example, the cities in a specific topographical basin were mostly assigned to a same group; thus, Huhehot and Datong which are both located on the northeastern margin of the Great Bend of the Yellow River were assigned to group G-3. On the other hand, cities located on different sides of a mountain were assigned to different groups, e.g. Shijiazhuang and Taiyuan which located on the east and the west of the Taihang Mountains are put into groups G-6 and G-3, respectively. Meanwhile, the cities in a same administrative prefecture (province) and those adjacent in geography were mostly assigned to the same group for the convenience of discussion.

Through these procedures, eighty-three cities in mid-eastern China (longitude 100° E to 130° E) are divided into fourteen groups (Fig. 1, Table 1). These groups generally correspond to the provincial regions. Three cities, Kelamayi (KLY), Urumchi (UMQ) and Lhasa (LS) located in western China were not included in these groups.

3 Results and discussion

3.1 Occurrences of the air quality categories

To better understand the spatial distribution of the air quality categories, the fourteen groups of the cities (Fig. 1, Table 1) were further partitioned into northern, middle and southern zones, with the Qinlin Mountain – the Huaihe River and the Yunnan-Guizhou Plateau – the Jiangnan Hill – the Wuyi Mountain as boundaries between zones (Fig. 3).

The northern and middle zones actually contain two basins oriented east/west while the southern zone is a hill area near the South China Sea and the East China Sea.

The percent occurrences of days with an air quality category of "clean" (API≤50) were greater than 17.4% for most of the cities in the southern zone (hereinafter referred to as the southern cities) but less than that for most of the middle and northern cities (Fig. 3a). Another feature of the data, which was to be expected, was that the occurrences of "clean" air quality were generally greater for the coastal cities compared with the inland cities (Fig. 3a). Figure 3b illustrates the percent occurrences of the days with air quality classification as "clean" or "good" (API≤100, that is, the air quality meet the Chinese National Grade II Ambient Air Quality Standard, CNAAQS-GII). One can see that in the southern zone, fifteen cities had air quality that met the CNAAQS-GII standard on more than 95% of the days. The exceptions to this were Guiyang, Liuzhou, Shaoguan and Guangzhou; in these four cities, less than 95% (but greater than 76.6%) of the days had air quality that met the standard.

Meanwhile in the northern zone, there were only six cities (four coastal cities: Dalian, Qinhuangdao, Yantai, Rizhao and two inland cities: Tai'an, Weifang) that had more than 95% of the days with air quality meet CNAAQS-GII (Fig. 3b). The cities with air qualities that most often meet CNAAQS-GII (percent occurrences of "clean" or "good" air quality greater than 76.6%, Fig. 3b) were restricted to the coastal area (six cities), Shandong Peninsula (five inland cities), and the remote Heilongjiang and Jilin Provinces (three and one cities, respectively). While for the other large area in the northern zone, most of the cities (18 of 23) had less than 76.6% (but greater than 50.3%) of the days when air quality met CNAAQS-GII (Fig. 3b).

For the cities in the middle zone, the percentages of the days on which air quality met CNAAQS-GII were intermediate between the northern and the southern zones (Fig. 3b). In contrast to the coastal cities in the other two zones, the occurrences of "clean" or "good" air quality for the coastal cities in the middle zone were all less than 95% (Fig. 3b). This was most likely due to intensive anthropogenic emissions caused by the rapid economic development in the Yangtze River Delta region (YRD), which

ACPD
9, 23141–23185, 2009

is in the coastal middle zone. Moreover, pollutants from both northern and southern areas may often transport over YRD and result in frequent deterioration of air quality.

The percent occurrences of days with air quality categorized as "low-level pollution" (100<API≤200) were larger for the northern cities than for those in the middle zone; these probabilities were lower for the cities in the southern zone (less than 10.6% except Liuzhou, Fig. 3c). Similar patterns can be seen for the occurrences of days with air quality categories of "mid- or high-level pollution" (API>200, Fig. 3d). Except for Guiyang and Guangzhou, which had relatively low occurrences "mid- or high-level pollution" (0.041% and 0.12%, respectively), these classifications never occurred in the southern zone.

Based on the API records, one would conclude that PM_{10} pollution is a greater concern than SO_2 and NO_2 because PM_{10} is the most common P_{prin} for Chinese cities (Table 3). One can see that for the northern zone and the southern zone, PM_{10} was P_{prin} on more than 80% of the days; while for the southern zone, about half of the days had PM_{10} as P_{prin} (and ~40% of the days with no P_{prin} reported). The percentages of days with SO_2 as P_{prin} ranged from 6.6% to 9.3% for the three latitudinal zones. In comparison, the numbers of days with NO_2 as P_{prin} were quite small but with relatively larger proportions for the southern zone (0.87%) compared with the northern and the southern zones (0.11% and 0.12%, respectively). This pattern in NO_2 as P_{prin} is probably due to more emissions from the motor vehicles in the south as well as more favorable conditions for the photochemical production of NO_2 in the southern zone.

3.2 Seasonal variations of the APIs and PM_{10}

High APIs most often occur during winter (December, January and February) and spring (March, April and May) while the lowest APIs are recorded during summer (June, July and August, Fig. 4). This is true for both the individual cities and the three zones. The seasonality in PM_{10} for the three latitudinal zones was similar to that of the APIs, i.e. with wintertime maxima and summertime minima (Table 4), but seasonal variability of PM_{10} in the southern zone was not so large as in the other zones. Meanwhile, high

ACPD
9, 23141–23185, 2009

springtime PM_{10} concentrations always followed the wintertime PM_{10} maxima (Table 4), and this is probably due to influence of dust events (Wang et al., 2004b). The exception is slightly lower PM_{10} levels in spring than autumn in the southern zone where the influence from dust events is weaker.

The seasonal variations in the APIs for the southern zone was not so evident as in the northern and middle zones, which can be clearly seen from the maximum APIs for the individual cities shown in Fig. 4. The maximum APIs commonly were around 500 during winter and spring for the cities in the northern zone (Fig. 4a), but they rarely (4 records) reached 500 for the cities in the middle zone (Fig. 4b). Continuing this trend, the maximum APIs for the cities in the southern zone were only about 300 for two days in autumn 2001 and 2003 (Fig. 4c).

Smaller seasonal variability of the APIs for the southern zone was probably due to weaker emissions in southern China compared with northern and middle China. For example, strong wintertime emissions from more heating as well as mineral aerosol from springtime dust storms impact the northern zone, and variations in sources such as these can undoubtedly result in strong seasonal variations in the APIs. In comparison, for the cities in southern China, there are less extensive domestic heating activities in winter as well as weaker influences of dust storms in spring.

However, accompanied with the implementation of the air quality improvement measures such as substituting natural gas for coal, controlling emissions from coal combustion, there is a dramatic increase of motor vehicles during the same course; the winter "heating season" pollution thus appears of minor importance in mega cities such as Beijing (Guinot et al., 2007). While the problem of air quality deterioration and visibility reduction tends to become more serious in summer during the high temperature and relative humidity weather conditions (Song et al., 2002); this meteorology always favors the photochemical production of secondary aerosol from precursor gases and the hygroscopic growth of the existing particles locally in the stagnation planetary boundary layer.

ACPD
9, 23141–23185, 2009

3.3 Influence of Asian dust on the APIs during spring

The number of springtime occurrences of the maximum API (=500) for the northern cities were about 30 for 2001 and 2002; this decreased to about 5 for 2003 through 2005, but steeply increased again to 22 during spring 2006 (top of Fig. 4a). Note the occurrences as tabulated here reflect the total number of days with API=500 for all cities in the northern zone, that is, if the API records reached 500 for more than one (e.g. *n*) city on a given day, the number of occurrences was tabulated as *n* for that day. The trend in the numbers of the days with API>300 for the northern cities during spring were similar to the occurrences of the API maxima, from 82 and 69 in 2001 and 2002, respectively, to about 12 for 2003 through 2005, then increasing again to 60 during spring 2006 (top of Fig. 4a).

The high APIs for the northern cities covaried with the frequencies of dust events, thus showing that the springtime air quality in northern China was degraded by Asian dust storms. The dust data used for this comparison are the frequencies of springtime dust storm events in northern China that were extracted by Zhang et al. (2008) from images taken with the Moderate Resolution Imaging Spectroradiometer (MODIS). Their study showed that there were 11, 8, 2, 3, 3 and 10 dust events in sequence from 2001 to 2006; and this measure of dust storm activity matches the interannual trend in the occurrence of the maximum APIs for the northern cities during spring (top of Fig. 4a). Li et al. (2007) also reported similar variation trend in frequencies of springtime dust events in Shijiazhuang city, which were 2, 0, 1, 2 and 3, respectively during 2002–2006. This tendency of the dust events frequency was also similar as those reported in Xi'an (Ning et al., 2005). Moreover, Wang et al. (2006) reported a severe influence of dust events on the variation of PM_{10} concentration over fourteen northern cities in China.

3.4 Spatial distribution of PM_{10}

Figure 5 illustrates the spatial distribution of PM_{10} for the 86 individual cities. Firstly, from the west to the east, the high PM_{10} regions and spots (arithmetic mean in $\mu g m^{-3}$)

ACPD
9, 23141–23185, 2009

in northern China included Urumchi (156.2) on the southern margin of the Junggar Basin, Lanzhou (192.1) and Xining (138.2) on the northeastern of the Qinghai-Tibetan Plateau, Weinan (151.5) and Xi'an (143.5) in the Guanzhong Basin, Taiyuan (178.5), Datong (162.4), Yangquan (152.9) and Changzhi (132.4) in Shanxi Province in the basins west of the Taihang Mountain, Pingdingshan (156.4, a coal industry city) and Kaifeng (133.1) in Henan Province on the western margin of the North China Plain, Beijing (159.2), Tianjin (139.9) and Shijiazhuang (167.7) in the northern part of the North China Plain, Jinan (135.1) in the eastern part of the North China Plain, Shenyang (144.8), Anshan (131.9) and Fushun (127.1) in the southeastern part of the Northeast China Plain. Secondly, in the middle zone, the high PM_{10} spots were Chongqing (141.8), Chengdu (120.3) and Luzhou (131.8) in the Sichuan Basin, Changsha (146.6) and Wuhan (135.4) in central China, Nanjing (125.1) and Hangzhou (119.1) in YRD. Finally, the PM_{10} levels in the cities in the southern zone were generally lower than those in the northern zone and the middle zone, and there was no spot with PM_{10} concentration $>109\,\mu g m^{-3}$ (Fig. 5). However, the average PM_{10} concentrations (in $\mu g m^{-3}$) were larger than 80 in four cities including Qujing (91.2), Guiyang (80.1), Guangzhou (84.7) and Shaoguan (86.5), which were much higher than the total average PM_{10} level of $58.2\,\mu g m^{-3}$ for the southern zone.

In general, the high PM_{10} regions and spots were consistent with areas and cities of dense population and intensive industrial activities. High PM_{10} concentration spots were documented in areas such as central-eastern China, the North China Plain, the Sichuan Basin, the Yangtze River Delta region (YRD) (Fig. 5), and the Pearl River Delta region (PRD, PM_{10} concentration $>80\,\mu g m^{-3}$), which were also identified as high AOD/AOT areas by the radiation/optical measurement and satellite observation studies (Luo et al., 2000, 2001; Li et al., 2003; Wang et al., 2008). At the same time, one should note that in a specific pollution episode, the situation of aerosol spatial distribution could differ largely from the averaged conditions as illustrated in Fig. 5.

Moreover, although the spatial distribution of PM_{10} was complicated, an overall north to south decreasing of PM_{10} level (latitudinal gradient) was distinct in Fig. 5, which will

ACPD
9, 23141–23185, 2009

be discussed in detail in Sect. 3.5.

The spatial distribution of PM_{10} concentration is not presented as an interpolated contour plot because the dataset is biased toward sites that are generally the most polluted "points" on a regional scale. That is, the cities typically are high-value centers in the field of PM_{10}, with low-value areas interspersed between these high PM_{10} loci. Although these results do not represent the full spatial distribution of the aerosol as done by the radiation/optical measurement network and satellite observation studies, they do provide important insights into the problems of air pollution *based on independent direct measurement of the surface air pollutant*.

Table 4 tabulates the arithmetic mean PM_{10} concentrations for the groups. Note these values tend to be less than the individual PM_{10} levels in mega cities because some "cleaner" small and satellite cities are included in the groups. From Table 4 one can see that in the northern zone, G-4 (corresponding to Heilongjiang and Jilin Provinces) and G-7 (Shandong Peninsula) exhibited significantly lower PM_{10} levels compared with other groups during spring, summer and autumn; while during winter, G-1 (Qinghai, Gansu and Ningxia Provinces), G-2 (Shaanxi Province), G-3 (Inner Mongolian and Shanxi Provinces) and G-5 (Liaoning Province) had significantly higher PM_{10} levels than other groups. For the three groups in the middle zone, G-9 (YRD) always showed the lowest PM_{10} concentration during four seasons. In the southern zone, PM_{10} levels were comparable for the three groups. For more detailed description of the seasonal patterns of PM_{10} spatial distribution, please see supplementary material 3 (http://www.atmos-chem-phys-discuss.net/9/23141/2009/acpd-9-23141-2009-supplement.zip).

3.5 Latitudinal gradient of PM_{10}

The PM_{10} concentrations for the northern zone were generally slightly higher than or comparable with those in the middle zone during spring, summer and autumn (Table 4). However, the wintertime PM_{10} concentrations in the northern zone were much higher than in the middle zone, presumably due to more emissions from domestic heating in

ACPD
9, 23141–23185, 2009

the colder northern zone and more intensive accumulation of pollutants near surface in the stable lower boundary layer (especially during nighttime). Along these lines, the median PM_{10} concentration at Urumchi during winter was 317 μgm^{-3}, which is about three times that in spring and autumn (92 μgm^{-3} and 116 μgm^{-3}, respectively), or more than five times that in summer (60 μgm^{-3}). This high aerosol loading at Urumchi indicates very severe wintertime particulate pollution in that city.

Overall, the PM_{10} concentrations in the southern zone were much lower (Table 4); they were only about half of those for the northern zone but more than half of those for the middle zone during all seasons. Although the PM_{10} concentrations showed a north-south difference in all the seasons, it was most pronounced in winter and less so in autumn (Table 4).

In addition to the distinct north to south decrease in PM_{10}, box and stem plots (Fig. 6) show patterns in PM_{10} variability; that is, both the concentrations and variability in PM_{10} were the lowest in the southern zone. The variabilities in PM_{10} in the northern zone were greater than the middle zone during spring, comparable during summer, but lower during autumn and winter. Another feature of the data is that the arithmetic mean PM_{10} concentrations are typically larger than the medians, especially for the northern zone and the middle zone (Fig. 6); this indicates that the PM_{10} concentrations were periodically elevated by pollution episodes.

The latitudinal gradient (north to south decrease) of PM_{10} levels was also confirmed by significant linear regressions ($p<0.0001$ significance) of PM_{10} median concentration with latitude of the cities (Fig. 7), one can see that there were generally lower PM_{10} levels in the southern cities than in the middle or northern cities. The reason and mechanism of the co-varying between the latitude and the PM_{10} loading remains unclear, but this latitudinal PM_{10} gradient between the three zones can be possibly explained by (1) more fossil fuel combustion for home heating during winter in the north, (2) stronger impacts from dust during spring for the cities in northern China, and (3) more efficient dilution of the pollutants by the prevailing clean maritime air and more efficient wet scavenging of the pariticles by the more abundant precipitation in southern

ACPD
9, 23141–23185, 2009

China. The slope of the regression fittings of PM_{10} concentration with latitude was the largest in winter, more than twofold those in summer and autumn (Fig. 7), indicating larger north to south PM_{10} gradient in winter.

Considering the large variability of the aerosols as a result of complex processes (emission, transport, photochemical transformation, deposition, and meteorological influence) and the complicated characteristics of the spatial distribution of PM_{10} (Fig. 5, Sect. 3.4), the latitudinal gradient in PM_{10} concentration just characterizes an overall feature regarding the spatial distribution of the urban aerosol in China. The latitudinal gradient of PM_{10} between these urban sites provides insights into the regional gradients of air pollution in mid-eastern China. The potential effects on climate and adverse health effects of this aerosol gradient need to be carefully evaluated as air pollution control strategies continue to be developed in China. At the same time, more detailed analysis of the spatial distribution of the atmospheric aerosol levels and compositions (e.g. from the MODIS satellite measurement) is obviously necessary in further assessment of the aerosols' climate effects.

3.6 Interannual variations in PM_{10}

As there were substantial changes in the sample size (number of cities) in June 2001, June 2004 and June 2006 (Table 1), only the 39 cities with full records (16, 11, and 12, respectively in the northern, middle and southern zone) were considered for the variation trend of PM_{10} in mid-eastern China during the study period (Fig. 8). A comparison between the entire dataset (all 83 cities in the three latitudinal zone) and the subset (39 cities with full records) indicated that they showed similar PM_{10} tendency, but the arithmetic means (or medians) of the subset were generally higher.

Figure 8 illustrates the interannual variation of the median PM_{10} concentrations for the three latitudinal zones during 2000–2006. For the northern zone, the springtime PM_{10} level decreased steeply from 157.0 $\mu g m^{-3}$ in 2001 to 123.0 $\mu g m^{-3}$ in 2002, and then fluctuated around 120 $\mu g m^{-3}$ from 2002 to 2006 with a minimum (108.3 $\mu g m^{-3}$) occurred in spring 2005 (Fig. 8a); the summertime PM_{10} level increased from 2000

ACPD
9, 23141–23185, 2009

to 2001, then decreased from 108.1 μgm^{-3} in 2001 to 82.8 μgm^{-3} in 2006 (Fig. 8b); the autumn PM_{10} level decreased steadily from 120.7 μgm^{-3} in 2000 to 94.4 μgm^{-3} in 2004, but then increased to about 100 μgm^{-3} during 2005–2006 (Fig. 8c); the wintertime PM_{10} level decreased obviously from 188.7 μgm^{-3} in 2000 to 135.6 μgm^{-3} in 2006, although with a few fluctuations during the course (Fig. 8d); the annual PM_{10} level (124.8 μgm^{-3} in 2000) increased firstly, then decreased from 136.0 μgm^{-3} in 2001 to about 101 μgm^{-3} during 2005–2006 (Fig. 8e). Because the springtime PM_{10} level can be elevated by the dust events, which may influence the variation trend in PM_{10}, the spring data was excluded to understand the influence of the anthropogenic emissions to the PM_{10} tendency. This kind of analysis showed that the summer, autumn and winter median PM_{10} level also decreased from about 124 μgm^{-3} during 2001–2002 to about 96 μgm^{-3} duirng 2005–2006 in the northern zone (Fig. 8f). In general, the PM_{10} level showed a decrease ($-23.2 \mu gm^{-3}$) for the northern cities from 2000 to 2006 (Fig. 8e).

On the other hand, because there were stringent and effective air pollution controlling efforts in Beijing before the 2008 Olympic Games, one may wonder the effect of these special air quality managements on the variation trend of PM_{10}. To clarify this issue, we excluded Beijing and the nearby cities (Tianjin and Shijiazhuang) from the trend analysis and inspected the PM_{10} tendency, which showed that although the PM_{10} levels were generally a little lower without these three cities, the variation trend was similar as the original. This suggested an ensemble decreasing trend in PM_{10} concentration for the cities in northern China, not just an achievement of temporary air quality improvement expedients for the Olympic Games.

For the middle zone, the springtime PM_{10} level varied similarly as that of the northern zone (Fig. 8a), which might reflect the influences of dust events. Moreover, for the middle zone, there was an overall decreasing trend of summertime PM_{10} concentration from 88.2 μgm^{-3} to 70.5 μgm^{-3} during the course, but with higher levels ($\sim 90 \mu gm^{-3}$) occurred during 2002–2004 (Fig. 8b); the autumn PM_{10} level increased

ACPD
9, 23141–23185, 2009

from 94.2 μgm^{-3} in 2000 to 128.2 μgm^{-3} in 2002, then decreased to ~108 μgm^{-3} during 2003–2004 and ~94 μgm^{-3} during 2005–2006 (Fig. 8c); the wintertime PM_{10} level fluctuated around 130 μgm^{-3} from 2000 to 2003, then decreased to a minimum (95.5 μgm^{-3}) in winter 2005 but increased to 125.8 μgm^{-3} in 2006 (Fig. 8d); the annual PM_{10} level fluctuated slightly around 100 μgm^{-3} during the course, from 98.7 μgm^{-3} in 2000 to 97.0 μgm^{-3} in 2006 (Fig. 8e); the summer, autumn and winter median PM_{10} level varied differently, firstly decreased from 98.7 μgm^{-3} in 2000 to 94.0 μgm^{-3} in 2001, then increased to ~107 μgm^{-3} during 2002–2003, but decreased again to a minimum of 88.9 μgm^{-3} in 2005, finally increased to 93.0 μgm^{-3} in 2006 (Fig. 8f). In general, the PM_{10} level in the middle zone fluctuated but showed unobvious change (−1.7 μgm^{-3}) during the course (Fig. 8e).

As for the southern zone, the springtime PM_{10} level fluctuated slightly with unobvious change during the course (59.4 μgm^{-3} in 2001 versus 59.3 μgm^{-3} in 2006, Fig. 8a); the summertime PM_{10} level decreased from 48.5 μgm^{-3} in 2000 to about 41 μgm^{-3} during 2001–2004, then increased to 45.8 μgm^{-3} in 2006 (Fig. 8b); the autumn PM_{10} level fluctuated around with an increase trend from 53.4 μgm^{-3} in 2000 to 65.2 μgm^{-3} in 2006 (Fig. 8c); the wintertime PM_{10} level fluctuated with an increase from 62.9 μgm^{-3} in 2000 to 72.9 μgm^{-3} in 2006 (Fig. 8d); the annual PM_{10} level fluctuated around with an increase trend from 53.3 μgm^{-3} in 2000 to 59.5 μgm^{-3} in 2006 (Fig. 8e); the summer, autumn and winter median PM_{10} level (Fig. 8f) varied similarly as the annual PM_{10} level (Fig. 8e). In general, the PM_{10} level in the southern zone fluctuated but showed a slight increase (+6.2 μgm^{-3}) during the course (Fig. 8e).

Taken together, in contrast to the slight increase (+6.2 μgm^{-3}) of PM_{10} concentration for the southern zone, the PM_{10} levels showed a decreasing trend (−23.2 μgm^{-3}) for the northern cities and a negligible decrease (−1.7 μgm^{-3}) for the middle zone during 2000 to 2006. This is a possible benefit of the country's implementation of more strict air pollution control strategies, such as reducing stationary emissions (cutting down small-scale coal-combustion electricity plants, migrating and managing heavy pollu-

ACPD
9, 23141–23185, 2009

tion industries – steel, metallurgy, chemical plants, etc.), substituting natural gas for coal, controlling mobile source emission from vehicles, improving road conditions and increasing urban vegetation coverage.

Several studies also have documented a decreasing trend of urban PM_{10} level and an improvement of urban air quality in northern and middle China. For example, Chan and Yao (2008) indicated that the annual median PM_{10} concentration in Beijing decreased from 180 $\mu g m^{-3}$ in 1999 to 142 $\mu g m^{-3}$ in 2005. A magnetics study in Lanzhou identified that the concentrations of magnetic minerals in the wintertime urban dustfall samples (collected during 1997–2005) have decreased, which indicated an improvement of the winter air quality (Xia et al., 2008). Zhang et al. (2006) also reported that the air quality in Shenyang was improved year by year from 1995 to 2004. In addition, PM_{10} concentration decreased dramatically from 146 $\mu g m^{-3}$ during January 2002–May 2003 (Wen et al., 2004) to 74.6±28.8 $\mu g m^{-3}$ during January 2006–February 2007 in Nanchong city. Shi et al. (2008) reported that the air quality has turned better in Shanghai, Nanjing, Hangzhou and Hefei from 2002 to 2005. Moreover, through statistic of more than 300 major cities in China, a recent research (Yao et al., 2009) indicated that the number percentage of the cities with PM_{10} concentrations less than 100 $\mu g m^{-3}$ increases from 36.8% to 62.8% during 2002 to 2006, while that of the cities with PM_{10} concentrations more than 150 $\mu g m^{-3}$ decreases steadily from 29.8% to 5.3%.

However, the aerosol burdens varied largely due to the interactions of many processes including emission (anthropogenic emission and natural dust release), transport (as well as convection influenced dispersion and dilution), photochemical transformation (new particle speciation and production of secondary aerosols), and deposition (dry and wet); meanwhile, there were also influences from the meteorology. The variation trend of the aerosols in China and its causes were more complicated and should be assessed cautiously; further study is obviously necessary on this issue.

3.7 Comparison of PM_{10} variation trend with AOD/AOT results

The decreasing trend of PM_{10} level in northern and middle China from 2000 to 2006 presented here seems to be different from the visibility decreasing tendency during a much longer period (1973–2007) identified by Wang et al. (2009). What has caused this inconsistency? In fact, an increasing trend of AOD was illustrated in detail in the authors' referred "*Asia (south)*" region (Fig. 1 in Wang et al., 2009), which includes not only China, but also the generally accepted south Asia area (Fig. S7 in the supporting online material of Wang et al., 2009, http://www.sciencemag.org/cgi/content/full/323/5920/1468/DC1). It is well known that the south Asia countries, such as India (Venkataraman et al., 2002), Pakistan (Smith et al., 1996), Bangladesh (Salam et al., 2003) and Vietnam (Deng et al., 2008b), experience severe air pollution problems; meanwhile, the AOD (0.55 μm) derived from visibility data of the meteorological stations during 2000–2007 was much higher over the south Asia countries (especially India and Bangladesh) than that over China (Fig. S1 in the supporting online material of Wang et al., 2009, http://www.sciencemag.org/cgi/content/full/323/5920/1468/DC1). If the heavily polluted south Asia was excluded from the referred "*Asia (south)*" region in Wang et al. (2009) and the AOD variation trend over China was inspected solely, the AOD tendency might be quite different. Moreover, these south Asia countries are also the usual source regions of the transboundary influx of air pollutants (including intensive biomass burning emission) to southwestern China and PRD (Deng et al., 2008b).

There was also inconsistency on the variation trend of AOD. According to emissions converted contributions to AOD, Streets et al. (2007) concluded that AOD over China has decreased from 1995–1996 (~0.305) to 2000 (0.29), which is consistent with the variation of surface shortwave irradiance measurements at 52 weather stations and the rise trend in mean surface temperatures in China starting about the middle of the 1990s. However, Xia et al. (2007) reported that AOD at 550 nm over Beijing increased from about 0.28 in 1980 to about 0.68 in 2005; using the Total Ozone Mapping Spec-

ACPD
9, 23141–23185, 2009

trometer (TOMS) monthly AOD at 500 nm data, Xie and Xia (2008) documented an increasing tendency of AOD in north China during 1997–2001, especially for the spring AOD in northeast China. This suggest that the characteristic and variation of AOD is complicated, which is determined not only by the anthropogenic emission and the natural material (dust, sea-salt, biogenic emission, etc.) contribution, but also by the influence of the vertical structure and height of the atmospheric mixing layer as well as the vertical profile of the aerosols' concentration and the composition. As year-to-year variability in meteorological conditions can influence input (of natural dust) from arid regions and input (of anthropogenic emission) from regional industrial and biomass burning sources (Guinot et al., 2007), this further complicated the issue. Further study is obviously necessary to figure out how much human activities have contributed to the AOD tendency and to identify the relationship between the AOD and the surface aerosol loading as well as the anthropogenic emission.

At the same time, it is worth noting that the variation in the surface PM_{10} concentration is not necessarily completely consistent with the variation trend of AOD (or AOT). Firstly, the AOD (or AOT) reflects the integrated optical property of the columnar atmospheric aerosol, which is strongly influenced by the vertical structure and height of the atmospheric mixing layer as well as the vertical profile of the aerosols' concentration and the composition; this is more complicated than characteristic of the surface aerosol. Secondly, it is the fine particles (e.g. $PM_{2.5}$, $PM_{1.0}$), whose sizes were closer to the wavelength range of the visible light, plays more important role in determining the aerosol optical property and in visibility impairing than the PM_{10}. That is, the AOD/AOT has stronger relationship with the fine particles than with the PM_{10}. For example, Bullrich (1964) indicated that the aerosol particles with diameter within 0.6–1.5 μm have the most effective impact on atmospheric extinction in the wavelength range of the visible light; a study in Beijing during June 1999 found that the submicron aerosol, although only contributed ~20% of the aerosol mass, was responsible for ~80% of the light scattering at 530 nm (Bergin et al., 2001); an investigation in Beijing during 1999–2000 showed a stronger relationship between the fine particle ($PM_{2.5}$) mass concen-

ACPD
9, 23141–23185, 2009

tration and the visibility degradation (Song et al., 2003); a research in Guangzhou also identified that the small scattering aerosol particles (<1 μm in radius) have the largest contribution (about 70%) to the reduction of visibility (Deng et al., 2008a).

Along these lines, Xia et al. (2006) found that the seasonal and diurnal variation of AOT in Beijing is quite different from that of surface particle concentration; AOT increases from January to June and then decreases gradually, while the PM_{10} concentration exhibits higher values in winter and spring and lower concentration in summer. Li et al. (2005) also reported that the seasonality of AOD over Urumchi was not entirely same as the variation in the concentration of the main pollutants such as PM_{10}, SO_2 and NO_2.

4 Conclusions

Most EPA-China's air quality monitoring stations are located in densely populated urban areas in middle-eastern China, and this is quite suitable for addressing concerns over the health effects of air pollution. However, to study the broader impacts of air pollution, such as climate effects, as well as to evaluate transboundary transport, more monitoring should be conducted at rural or remote sites, especially in western China and along the country's borders. At the same time, specific types of air pollutants with the potential to influence climate (e.g. radiative forcing), such as black carbon, sulfate and dust aerosol should be included in the monitoring programs.

The latitudinal gradient in PM_{10} concentration presented here just characterizes an overall feature of the urban aerosol distribution in China. The spatial distribution of the atmospheric aerosols was more complicated than this. In further assessment of the aerosols' climate effects, more detailed investigation and study on the spatial distribution of the atmospheric aerosols' concentration and composition were essential.

Besides the latitudinal gradient documented above, a distinct longitudinal aerosol gradient is evident in the northern zone where PM_{10} concentrations decreased from west to east (please see supplementary material 2 http://www.atmos-chem-phys-discuss.net/9/23141/2009/acpd-9-23141-2009-supplement.zip).

ACPD
9, 23141–23185, 2009

A strong west-to-east gradient of BC along the latitude lines of 30° N and 35° N also has been observed over the central Pacific Ocean (Kaneyasu and Murayama, 2000). Weaker influences from desert dust and anthropogenic pollutants as well as more efficient dilution with relatively clean marine air likely contribute to low PM_{10} levels in the eastern cities in northern China. On the other hand, for the cities in the middle and southern zones, PM_{10} concentrations also generally exhibited a decreasing trend from west to east, but the longitudinal differences in those cases were smaller and insignificant.

The frequencies of Asian dust events mirrored the API maxima for the northern cities, and this indicates that dust can contribute to the degradation of springtime air quality in northern China. Along the same lines, Li et al. (2007) identified important influence of dust events on spring air quality in Shijiazhuang city during 2002–2006, when all of the springtime days with mid-level or more serious pollution were the concurrent or following days of the dust-events. Wang et al. (2004b) also reported a significant contribution of Asian dust to PM_{10} pollution at Beijing during the springtime. This is significant because desert dust production will be difficult if not impossible to control, and some allowances for naturally-occurring PM may be appropriate for air quality standards.

The API data show that PM_{10} is most often the P_{prin}, but the records of SO_2 and NO_2 are discontinuous, and a more complete assessment of their spatial distribution and temporal trends requires the collection of more data. NO_2 was reported as P_{prin} on only ~0.3% of the APIs recorded days. However, as the number of motor vehicles in China increases and the country's efforts to control emissions of particulates and SO_2 expand, the situation is likely to change. Changes in energy sources during the course of economic development also will influence the mix of pollutants. A study in Beijing found that the winter "heating season" appears of minor importance at present, whereas traffic is likely to dominate downtown anthropogenic emissions in the future (Guinot et al., 2007). Therefore, NO_χ pollution may become increasingly important in China, and along with continued monitoring, effective strategies should be imple-

ACPD
9, 23141–23185, 2009

mented to control NO_χ emissions (Hao and Tian, 2003).

Acknowledgements. The daily API records for 86 Chinese cities are obtained from State Environmental Protection Agency of China (http://www.sepa.gov.cn/quality/air.php3). This research was supported by National Basic Research Program of China (Grant No. 2006CB403701, 2006CB403702), the Chinese Ministry of Education's 111 Project (B07036) and by the National Science Foundation of the United States (ATM 0404944).

References

Bari, A., Ferraro, V., Wilson, L. R., Luttinger, D., and Husain, L.: Measurements of gaseous HONO, HNO_3, SO_2, HCl, NH_3, particulate sulfate and $PM_{2.5}$ in New York, NY, Atmos. Environ., 37(20), 2825–2835, 2003.

Bergin, M. H., Cass, G. R., Xu, J., Fang, C., Zeng, L. M., Yu, T., Salmon, L. G., Kiang, C. S., Tang, X. Y., Zhang, Y. H., and Chameides, W. L.: Aerosol radiative, physical, and chemical properties in Beijing during June 1999, J. Geophys. Res., 106(D16), 17969–17980, 2001.

Bi, X. H., Feng, Y. C., Wu, J. H., Wang, Y. Q., and Zhu, T.: Source apportionment of PM_{10} in six cities of northern China, Atmos. Environ., 41, 903–912, 2007.

Bullrich, K.: Scattered radiation in the atmosphere and the natural aerosol, Adv. Geophys., 10, 99–258, 1964.

Cao, J. J., Lee, S. C., Ho, K. F., Zhang, X. Y., Zou, S. C., Fung, K., Chow, J. C., and Watson, J. G.: Characteristics of carbonaceous aerosol in Pearl River Delta Region, China during 2001 winter period, Atmos. Environ., 37, 1451–1460, 2003.

Chan, C. K. and Yao, X. H.: Air pollution in mega cities in China, Atmos. Environ., 42, 1–42, 2008.

Charlson, R. J., Schwartz, S. E., Hales, J. M., Cess, R. D., Coakley, J. A. J., Hansen, J. E., and Hofmann, D. J.: Climate forcing by anthropogenic aerosols, Science, 255, 423–430, 1992.

Chu, P. C., Chen, Y. C., Lu, S. H., Li, Z. C., and Lu, Y. Q.: Particulate air pollution in Lanzhou China, Environ. Int., 34, 698–713, 2008.

Collins, D. R., Jonsson, H. H., Liao, H., Flagan, R. C., Seinfeld, J. H., Noone, K. J., and Hering, S. V.: Airborne analysis of the Los Angeles aerosol, Atmos. Environ., 34, 4155–4173, 2000.

Davis, B. L. and Guo, J. X.: Airborne particulate study in five cities of China, Atmos. Enviro., 34, 2703–2711, 2000.

Deng, X. J., Tie, X. X., Wu, D., Zhou, X. J., Bi, X. Y., Tan, H. B., Li, F., and Jiang, C. L.: Long-term trend of visibility and its characterizations in the Pearl River Delta (PRD) region, China, Atmos. Environ., 42, 1424–1435, 2008a.

Deng, X. J., Tie, X. X., Zhou, X. J., Wu, D., Zhong, L. J., Tan, H. B., Li, F., Huang, X. Y., Bi, X. Y., and Deng, T.: Effects of Southeast Asia biomass burning on aerosols and ozone concentrations over the Pearl River Delta (PRD) region, Atmos. Environ., 42, 8493–8501, 2008b.

Duan, F. K., He, K. B., Ma, Y. L., Jia, Y. T., Yang, F. M., Lei, Y., Tanaka, S., and Okuta, T.: Characteristics of carbonaceous aerosols in Beijing, China, Chemosphere, 60, 355–364, 2005.

Fang, M., Zheng, M., Wang, F., Chim, K. S., and Kot, S. C.: The long-range transport of aerosols from northern China to Hong Kong – a multi-technique study, Atmos. Environ., 33, 1803–1817, 1999.

Feng, J. L., Hu, M., Chan, C. K., Lau, P. S., Fang, M., He, L. Y., and Tang, X. Y.: A comparative study of the organic matter in $PM_{2.5}$ from three Chinese megacities in three different climatic zones, Atmos. Environ., 40, 3983–3994, 2006.

Guinot, B., Cachier, H., Sciare, J., Tong, Y., Xin, W., and Jianhua, Y.: Beijing aerosol: Atmospheric interactions and new trends, J. Geophys. Res., 112, D14314, doi:10.1029/2006JD008195, 2007.

Hao, J. M. and Tian, H. Z.: Status, trend and control strategy proposal of NO_χ emissions in China, in: Symposium of NO_χ Pollution Control in China, edited by: Chinese Society for Environmental Sciences, Chinese Society for Environmental Sciences, Beijing, 8–19, 2003 (in Chinese).

He, K. B., Yang, F. M., Ma, Y. L., Zhang, Q., Yao, X. H., Chan, C. K., Cadle, S., Chan, T., and Mulawa, P.: The characteristics of $PM_{2.5}$ in Beijing, China, Atmos. Environ., 35, 4959–4970, 2001.

Highwood, E. J. and Kinnersley, R. P.: When smoke gets in our eyes: The multiple impacts of atmospheric black carbon on climate, air quality and health, Environ. Int., 32, 560–566, 2006.

Kaneyasu, N. and Murayama, S.: High concentrations of black carbon over middle latitudes in the North Pacific Ocean, J. Geophys. Res., 105(D15), 19881–19890, 2000.

Kaufman, Y. J., Tanre, D., and Boucher, O.: A satellite view of aerosols in the climate system, Nature, 419, 215–223, 2002.

ACPD

9, 23141–23185, 2009

King, A. M.: New directions: TEOMs and the volatility of UK non-urban PM_{10}: a regulatory dilemma?, Atmos. Environ., 34, 3210–3212, 2000.
Li, C. C., Mao, J. T., Lau, K. A., Chen, J. C., Yuan, Z. B., Liu, X. Y., Zhu, A. H., and Liu, G. Q.: Characteristics of distribution and seasonal variation of aerosol optical depth in eastern China with MODIS products, Chinese Sci. Bull., 48(22), 2488–2495, 2003.
Li, G. C., Wang, J. G., and Lian, Z. L.: Relationship between atmospheric pollution and sandy weather in Shijiazhuang, Journal of Meteorology and Environment, 23(2), 1–5, 2007 (in Chinese with English abstract).
Li, J., Zhuang, G. S., Huang, K., Lin, Y. F., Xu, C., and Yu, S. L.: Characteristics and sources of air-borne particulate in Urumqi, China, the upstream area of Asia dust, Atmos. Environ., 42, 776–787, 2008.
Li, S.-M., Tang, J., Xue, H., and Toom-Sauntry, D.: Size distribution and estimated optical properties of carbonate, water soluble organic carbon, and sulfate in aerosols at a remote high altitude site in Western China, Geophys. Res. Lett., 27(8), 1107–1110, 2000.
Li, X., Chen, Y. H., Hu, X. Q., Ren, Y. Y., and Wei, W. S.: Analysis of atmospheric aerosol optical properties over Urumqi, China Environmental Science, 25 (supp.), 22–25, 2005 (in Chinese with English abstract).
Li, Y., Zhang, X. Y., Gong, S. L., Che, H. Z., Wang, D., Qu, W. J., and Sun, J. Y.: Comparison of EC and BC and evaluation of dust aerosol contribution to light absorpition in Xi'An, China, Environ. Monit. Assess., 120, 301–312, 2006.
Luo, Y. F., Lü, D. R., He, Q., Li, W. L., and Zhou, X. J.: Characteristics of atmospheric aerosol optical depth variation over China in recent 30 years, Chinese Sci. Bull., 45(14), 1328–1333, 2000.
Luo, Y., Lu, D., Zhou, X., Li, W., and He, Q.: Characteristics of the spatial distribution and yearly variation of aerosol optical depth over China in last 30 years, J. Geophys. Res., 106(D13), 14501–14513, 2001.
Meng, Z. Y., Jiang, X. M., Yan, P., Lin, W. L., Zhang, H. D., and Wang, Y.: Characteristics and sources of $PM_{2.5}$ and carbonaceous species during winter in Taiyuan, China, Atmos. Environ., 41, 6901–6908, 2007.
Met One Instruments Inc: BAM-1020 continuous particulate monitor: http://www.metone.com/documents/BAM-1020_6-08.pdf, access: 28 Aug 2009.
Meywerk, J. and Ramanathan, V.: Observations of the spectral clear-sky aerosol forcing over the tropical Indian Ocean, J. Geophys. Res., 104(D20), 24359–24370, 1999.

Mo, Y. C., Zheng, F. Q., and Liao, G. L.: Correlation analysis of PM_{10} concentration and meteorological condition in Nanning, Journal of Meteorological Research and Application, 29(1), 55–56, 2008 (in Chinese with English abstract).

Nair, V. S., Babu, S. S., and Moorthy, K. K.: Aerosol characteristics in the marine atmospheric boundary layer over the Bay of Bengal and Arabian Sea during ICARB: Spatial distribution and latitudinal and longitudinal gradients, J. Geophys. Res., 113, D15208, doi:10.1029/2008JD009823, 2008.

Ning, H. W., Wang, S. G., and Du, J. W.: Characteristics of sand-dust events and their influence on air quality of Xi'an city, Journal of Desert Research, 25(6), 886–890, 2005 (in Chinese with English abstract).

Okuda, T., Kato, J., Mori, J., Tenmoku, M., Suda, Y., Tanaka, S., He, K. B., Ma, Y. L., Yang, F. M., Yu, X. C., Duan, F. K., and Lei, Y.: Daily concentrations of trace metals in aerosols in Beijing, China, determined by using inductively coupled plasma mass spectrometry equipped with laser ablation analysis, and source identification of aerosols, Sci. Total Environ., 330, 145–158, 2004.

Okuda, T., Katsuno, M., Naoi, D., Nakao, S., Tanaka, S., He, K. B., Ma, Y. L., Lei, Y., and Jia, Y. T.: Trends in hazardous trace metal concentrations in aerosols collected in Beijing, China from 2001 to 2006, Chemosphere, 72, 917–924, 2008.

Pope, C. A., Dockery, D. W., and Schwartz, J.: Review of epidemiological evidence of health effects of particulate air pollution, Inhal. Toxicol., 7, 1–18, 1995.

Qu, W. J., Zhang, X. Y., Arimoto, R., Wang, D., Wang, Y. Q., Yan, L. W., and Li Y.: Chemical composition of the background aerosol at two sites in southwestern and northwestern China: potential influences of regional transport, Tellus B, 60, 657–673, 2008.

Rajeev, K. and Ramanathan, V.: Direct observations of clear-sky aerosol radiative forcing from space during the Indian Ocean Experiment, J. Geophys. Res., 106(D15), 17221–17235, 2001.

Salam, A., Bauer, H., Kassin, K., Ullah, S. M., and Puxbaum, H.: Aerosol chemical characteristics of a mega-city in Southeast Asia (Dhaka-Bangladesh), Atmos. Environ., 37, 2517–2528, 2003.

Shi, C. E., Zhai, W. Q., Yang, J., Wang, S., and Yao, K. Y.: Characteristics of PM_{10} pollution at four provincial cities in Yangtze River Delta district, Plateau Meteorology, 27(2), 408–414, 2008 (in Chinese with English abstract).

Smith, D. J. T., Harrision, R. M., Luhana, L., Casimiro, A. P., Castro, L. M., Tariq, M. N., Hayat,

S., and Quraishi, T.: Concentrations of particulate airborne polycyclic aromatic hydrocarbons and metals collected in Lahore, Pakistan, Atmos. Environ., 30, 4031–4040, 1996.
Song, Y., Tang, X. Y., Zhang, Y. H., Hu, M., Fang, C., Zen, L. M., and Wang, W.: Effects on fine particles by the continued high temperature weather in Beijing, Environm. Sci., 23(4), 33–36, 2002 (in Chinese with English abstract).
Song, Y., Tang, X. Y., Fang, C., Zhang, Y. H., Hu, M., Zeng, L. M., Li, C. C., Mao, J. T., and Bergin, M.: Relationship between the visibility degradation and particle pollution in Beijing, Acta Scientiae Circumstantiae, 23(4), 468–471, 2003 (in Chinese with English abstract).
Streets, D. G., Yu, C., Wu, Y., Chin, M., Zhao, Z. C., Hayasaka, T., and Shi, G. Y.: Did Aerosols over China peak in the 1990s?, discussion paper of Global Environment and Energy in the 21st Century: http://www.gee-21.org/publications/pdf%20files/StreetsetalAerosolsoverChinaJan2007.pdf, available: 2007.
Ta, W. Q., Wang, T., Xiao, H. L., Zhu, X. Y., and Xiao, Z.: Gaseous and particulate air pollution in the Lanzhou Valley, China, Sci. Total Environ., 320, 163–176, 2004.
Tang, J., Wen, Y. P., Zhou, L. X., Qi, D. L., Zheng, M., Trivett, N., and Wallgren, E.: Observational study of black carbon in clean air area of western China, Quarterly Journal of Applied Meteorology, 10(2), 160–170, 1999 (in Chinese with English abstract).
Twomey, S.: The influence of pollution on the short-wave albedo of clouds, J. Atmos. Sci., 34, 1149, 1977.
Venkataraman, C., Reddy, C. K., Josson, S., and Reddy, M. S.: Aerosol size and chemical characteristics at Mumbai, India, during the INDOEX-IFP (1999), Atmos. Environ., 36, 1979–1991, 2002.
Wang, K. C., Dickinson, R. E., and Liang, S. L.: Clear sky visibility has decreased over Land globally from 1973 to 2007, Science, 323, 1468–1470, 2009.
Wang, S. G., Wei, Y., and Shang, K. Z.: The impacts of different kinds of dust events on PM_{10} pollution in northern China, Atmos. Environ., 40, 7975–7982, 2006.
Wang, T., Wong, C. H., Cheung, T. F., Blake, D. R., Arimoto, R., Baumann, K., Tang, J., Ding, G. A., Yu, X. M., Li, Y. S., Streets, D. G., and Simpson, I. J.: Relationships of trace gases and aerosols and the emission characteristics at Lin'an, a rural site in eastern China, during spring 2001, J. Geophys. Res., 109, D19S05, doi:10.1029/2003JD004119, 2004a.
Wang, Y., Xin, J., Li, Z., Wang, S., Wang, P., Hao, W. M., Nordgren, B. L., Chen, H., Wang, L., and Sun, Y.: Seasonal variations in aerosol optical properties over China, Atmos. Chem. Phys. Discuss., 8, 8431–8453, 2008,

http://www.atmos-chem-phys-discuss.net/8/8431/2008/.
Wang, Y. Q., Zhang, X. Y., Arimoto, R., Cao, J. J., and Shen, Z. X.: The transport pathways and sources of PM_{10} pollution in Beijing during spring 2001, 2002 and 2003, Geophys. Res. Lett., 31, L14110, doi:10.1029/2004GL019732, 2004b.
Watson, J.: Visibility: Science and regulation, J. Air Waste Manage. Assoc., 52, 628–713, 2002.
Wen, X. H., He, P., Li, C. Z., and Luo, X. Y.: Pollution level of the airborne particulate matter (PM_{10}) in Nanchong City, Sichuan Environment, 23(2), 72–74, 2004 (in Chinese with English abstract).
Wu, D., Tie, X. X., Li, C. C., Ying, Z. M., Lau, A. K., Huang, J., Deng, X. J., and Bi, X. Y.: An extremely low visibility event over the Guangzhou region: A case study, Atmos. Environ., 39, 6568–6577, 2005.
Xia, D. S., Chen, F. H., Bloemendal, J., Liu, X. M., Yu, Y., and Yang, L. P.: Magnetic properties of urban dustfall in Lanzhou, China, and its environmental implications, Atmos. Environ., 42, 2198–2207, 2008.
Xia, X. A., Chen, H. B., Wang, P. C., Zhang, W. X., Goloub, P., Chatenet, B., Eck, T. F., and Holben, B. N.: Variation of column-integrated aerosol properties in a Chinese urban region, J. Geophys. Res., 111, D05204, doi:10.1029/2005JD006203, 2006.
Xia, X., Chen, H., Goloub, P., Zhang, W., Chatenet, B., and Wang, P.: A compilation of aerosol optical properties and calculation of direct radiative forcing over an urban region in northern China, J. Geophys. Res., 112, D12203, doi:10.1029/2006JD008119, 2007.
Xie, J. X., and Xia, X. A.: Long-term trend in aerosol optical depth from 1980 to 2001 in north China, Particuology, 6, 106–111, 2008.
Xu, J., Bergin, M. H., Yu, X., Liu, G., Zhao, J., Carrico, C. M., and Baumann, K.: Measurement of aerosol chemical, physical and radiative properties in the Yangtze delta region of China, Atmos. Environ., 36, 161–173, 2002.
Yao, Q., Li, S. Q., Xu, H. W., Zhuo, J. K., and Song, Q.: Studies on formation and control of combustion particulate matter in China: A review, Energy, 34(9), 1296–1309, 2009.
Ye, B. M., Ji, X. L., Yang, H. Z., Yao, X. H., Chan, C. K., Cadle, S. H., Chan, T., and Mulawa, P. A.: Concentration and chemical composition of $PM_{2.5}$ in Shanghai for a 1-year period, Atmos. Environ., 37(4), 499–510, 2003.
Zhang, B. L., Tsunekawa, A., and Tsubo, M.: Contributions of sandy lands and stony deserts to long-distance dust emission in China and Mongolia during 2000–2006, Global Planet.

Change, 60, 487–504, 2008.
Zhang, X. M., Chai, F. H., Wang, S. L., Hu, B. Q., Li, K., and Luo, L. B.: Characteristics of air pollution in Shenyang city, China, China Environmental Science, 26(6), 650–652, 2006 (in Chinese with English abstract).
Zhang, X. Y., Cao, J. J., Li, L. M., Arimoto, R., Cheng, Y., Huebert, B., and Wang, D.: Characterization of atmospheric aerosol over XiAn in the South Margin of the Loess Plateau, China, Atmos. Environ., 36, 4189–4199, 2002.
Zhang, X. Y., Gong, S. L., Shen, Z. X., Mei, F. M., Xi, X. X., Liu, L. C., Zhou, Z. J., Wang, D., Wang, Y. Q., and Cheng, Y.: Characterization of soil dust aerosol in China and its transport/distribution during 2001 ACE-Asia: 1. Network observations, J. Geophys. Res., 108(D9), 4261, doi:10.1029/2002JD002632, 2003.
Zhang, X. Y., Wang, Y. Q., Wang, D., Gong, S. L., Arimoto, R., Mao, L. J., and Li, J.: Characterization and sources of regional-scale transported carbonaceous and dust aerosols from different pathways in coastal and sandy land areas of China, J. Geophys. Res., 110, D15301, doi:10.1029/2004JD005457, 2005.
Zheng, M., Salmon, L. G., Schauer, J. J., Zeng, L. M., Kiang, C. S., Zhang, Y. H., and Cass, G. R.: Seasonal trends in $PM_{2.5}$ source contributions in Beijing, China, Atmos. Environ., 39(22), 3967–3976, 2005.

Table 1. Locations, groups and air pollution index (API) data available period of the 86 cities in China.

Group (Representative area)	City	Latitude, Longitude	API data available period[a]
G-1	Xining (XN)	36.62° N, 101.82° E	A
(Qinghai,	Shizuishan (SZS)	39.02° N, 106.22° E	C
Gansu and	Yinchuan (YC)	38.47° N, 106.22° E	A
Ningxia Province)	Lanzhou (LaZ)	36.05° N, 103.83° E	A
G-2	Baoji (BaJ)	34.35° N, 107.15° E	C
(Shaanxi Province)	Xi'an (XA)	34.25° N, 108.92° E	A
	Weinan (WN)	34.30° N, 109.30° E	C
G-3	Hohehot (HHT)	40.80° N, 111.63° E	A
(Inner Mongolian	Chifeng (CF)	42.17° N, 118.58° E	C
and Shanxi	Datong (DT)	40.12° N, 113.22° E	C
Province)	Taiyuan (TY)	37.85° N, 112.55° E	A
	Yangquan (YQ)	37.51° N, 113.34° E	C
	Changzhi (CZ)	36.08° N, 113.22° E	C
G-4	Qiqihar (QHR)	47.37° N, 123.92° E	C
(Heilongjiang	Harbin (HRB)	45.75° N, 126.63° E	A
and Jilin Province)	Mudanjiang (MDJ)	44.58° N, 129.60° E	C
	Changchun (CC)	43.92° N, 125.30° E	A
G-5	Fushun (FS)	41.51° N, 123.54° E	C
(Liaoning	Shenyang (SY)	41.80° N, 123.38° E	A
Province)	Anshan (AS)	41.06° N, 123.00° E	C
G-6	Beijing (BeJ)	39.90° N, 116.47° E	A
(Beijing, Tianjin,	Tianjin (TJ)	39.17° N, 117.17° E	A
Hebei Province	Shijiazhuang (SJZ)	38.05° N, 114.43° E	A
and Dalian City)	Qinhuangdao (QHD)	39.90° N, 119.62° E	B
	Dalian (DL)	38.90° N, 121.63° E	B
G-7	Yantai (YT)	37.55° N, 121.33° E	A
(Shandong	Qingdao (QD)	36.07° N, 120.32° E	A
Province and	Rizhao (RZ)	35.23° N, 119.32° E	C
Lianyungang City)	Lianyungang (LYG)	34.59° N, 119.16° E	B
	Weifang (WF)	36.43° N, 119.06° E	C
	Zibo (ZB)	36.48° N, 118.03° E	C
	Jinan (JNa)	36.67° N, 117.03° E	A
	Tai'an (TA)	36.11° N, 117.08° E	C
	Zaozhuang (ZZh)	34.52° N, 117.33° E	C
	Jining (JNi)	35.23° N, 116.33° E	C

ACPD
9, 23141–23185, 2009

Table 1. Continued.

Group (Representative area)	City	Latitude, Longitude	API data available period[a]
G-8	Kaifeng (KF)	34.87° N, 114.38° E	C
(Henan Province)	Zhengzhou	34.73° N, 113.70° E	A
	Pingdingshan	33.44° N, 113.17° E	C
G-9	Hefei (HF)	31.85° N, 117.27° E	A
(Shanghai,	Wuhu (WHu)	31.35° N, 118.33° E	C
Anhui,	Nanjing (NJ)	32.05° N, 118.77° E	A
Jiangsu,	Yangzhou (YZ)	32.23° N, 119.26° E	C
and Zhejiang	Zhenjiang (ZheJ)	32.11° N, 119.27° E	C
Province)	Nantong (NT)	32.01° N, 120.51° E	A
	Suzhou (SZ)	31.33° N, 120.65° E	A
	Shanghai (SH)	31.20° N, 121.43° E	A
	Huzhou (HuZ)	30.52° N, 120.06° E	C
	Hangzhou (HaZ)	30.25° N, 120.17° E	A
	Shaoxing (SX)	30.00° N, 120.34° E	C
	Ningbo (NB)	29.88° N, 121.57° E	B
G-10	Jiujiang (JJ)	29.72° N, 115.98° E	C
(Jiangxi, Hubei	Nanchang (NCha)	28.68° N, 115.88° E	A
and Hunan	Wuhan (WHa)	30.62° N, 114.33° E	A
Province)	Jingzhou (JZ)	30.33° N, 112.18° E	C
	Changsha (CS)	28.20° N, 112.92° E	A
	Changde (ChaD)	29.00° N, 111.65° E	C
	Zhangjiajie (ZJJ)	29.08° N, 110.29° E	C
G-11	Nanchong (NCho)	30.49° N, 106.04° E	D
(Chongqing and	Chongqing (CQ)	29.55° N, 106.55° E	A
Sichuan Province)	Luzhou (LuZ)	28.90° N, 105.45° E	C
	Zigong (ZG)	29.23° N, 104.46° E	D
	Chengdu (CheD)	30.65° N, 104.07° E	A
	Deyang (DY)	31.09° N, 104.22° E	C
	Mianyang (MY)	31.30° N, 104.42° E	C

ACPD
9, 23141–23185, 2009

Table 1. Continued.

Group (Representative area)	City	Latitude, Longitude	API data available period[a]
G-12	Qujing (QJ)	25.30° N, 103.48° E	C
(Yunnan Province)	Kunming (KM)	25.05° N, 102.70° E	A
	Yuxi (YX)	24.22° N, 102.32° E	C
G-13	Guiyang (GY)	26.57° N, 106.72° E	A
(Guangxi,	Guilin (GL)	25.30° N, 110.17° E	B
Guizhou,	Liuzhou (LiZ)	24.33° N, 109.32° E	C
Hainan Province	Nanning (NN)	22.78° N, 108.35° E	A
and	Beihai (BH)	21.28° N, 109.07° E	B
Zhanjiang City)	Zhanjiang (ZhaJ)	21.11° N, 110.24° E	A
	Haikou (HK)	20.05° N, 110.17° E	A
G-14	Shaoguan (SG)	24.80° N, 113.55° E	C
(Guangdong,	Guangzhou (GZ)	23.17° N, 113.30° E	A
Fujian Province	Zhuhai (ZH)	22.17° N, 113.34° E	A
and Wenzhou Ciy)	Shenzhen (ShZ)	22.33° N, 114.07° E	A
	Shantou (ST)	23.35° N, 116.67° E	A
	Xiamen (XM)	24.43° N, 118.07° E	A
	Quanzhou (QZ)	24.90° N, 118.62° E	C
	Fuzhou (FZ)	26.03° N, 119.32° E	A
	Wenzhou (WZ)	28.00° N, 120.63° E	A
	Kelamayi (KLY)	45.36° N, 84.51° E	C
	Urumchi (UMQ)	43.77° N, 87.60° E	A
	Lhasa (LS)	29.65° N, 91.03° E	A

[a] Here API data available period was denoted by A: from June 2000 to February 2007, B: from June 2001 to February 2007, C: from June 2004 to February 2007, and D: from January 2006 to February 2007.

ACPD

9, 23141–23185, 2009

Table 2. Air quality classifications corresponding to the air pollution indexes (APIs), air quality management recommendations, and pollutant concentrations in China.

Air pollution index (API)	Air quality classification		Air quality management recommendation	Corresponding daily averaged pollutants' concentration, μgm^{-3}		
				PM_{10}	SO_2	NO_2
API≤50	I	Clean	No action is needed.	$PM_{10}\leq 50$	$SO_2\leq 50$	$NO_2\leq 80$
50<API≤100	II	Good	No action is needed.	$50<PM_{10}\leq 150$	$50<SO_2\leq 150$	$80<NO_2\leq 120$
100<API≤150	III_1	Low-level pollution	Persons should be careful in outdoor activities.	$150<PM_{10}\leq 250$	$150<SO_2\leq 475$	$120<NO_2\leq 190$
150<API≤200	III_2			$250<PM_{10}\leq 350$	$475<SO_2\leq 800$	$190<NO_2\leq 280$
200<API≤250	IV_1	Mid-level pollution	Persons with existing heart or respiratory illnesses are advised to reduce physical exertion and outdoor activities.	$350<PM_{10}\leq 385$	$800<SO_2\leq 1200$	$280<NO_2\leq 422.5$
250<API≤300	IV_2			$385<PM_{10}\leq 420$	$1200<SO_2\leq 1600$	$422.5<NO_2\leq 565$
300<API≤500	V	High-level pollution	Air pollution is severe; The general public is advised to reduce physical exertion and outdoor activities.	$420<PM_{10}\leq 600$	$1600<SO_2\leq 2600$	$565<NO_2\leq 940$

ACPD
9, 23141–23185, 2009

Table 3. The Proportions of days with PM_{10}, SO_2 and NO_2 as the principal pollutant in the whole air pollution index (API) records for the 14 groups and 3 latitudinal zones.

Group/Zone (City)	Proportion in the whole API records[a] Days with PM_{10} as the principal pollutant	Days with no principal pollutant reported (API≤50)	Days with SO_2 as the principal pollutant	Days with NO_2 as the principal pollutant
G-1	85.8	5.6	8.5	0.036
G-2	96.0	1.9	2.0	
G-3	78.5	6.7	14.2	0.68
G-4	89.7	9.7	0.5	0.12
G-5	91.7	2.1	6.3	
G-6	76.5	9.1	14.4	
G-7	77.8	14.4	7.8	
G-8	92.7	3.5	3.8	0.045
Northern Zone[b]	**83.2**	**8.3**	**8.4**	**0.11**
G-9	81.2	17.4	1.2	0.22
G-10	81.6	8.6	9.9	
G-11	76.1	7.9	16.0	0.011
Middle Zone	**80.2**	**13.0**	**6.6**	**0.12**
G-12	68.4	15.8	15.8	
G-13	32.1	53.3	14.6	
G-14	58.3	36.3	3.6	1.8
Southern Zone	**49.3**	**40.6**	**9.3**	**0.87**
Kelamayi	54.5	45.5		
Urumchi	69.4	15.2	15.4	0.041
Lhasa	59.2	40.8		

[a] Proportion in percentage (%).

[b] The three latitudinal zones are same as those illustrated in Fig. 2.

ACPD

9, 23141–23185, 2009

Table 4. Seasonal arithmetic mean PM_{10} concentrations for the 14 groups and 3 latitudinal zones.

Group/Zone (City)	Arithmetic mean ± Standard deviation[a] (n[b]) Whole study period	Spring	Summer	Autumn	Winter
G-1	139.3±75.3 (2451)	164.8±98.6 (552)	94.5±28.4 (640)	119.0±48.7 (637)	183.4±73.8 (622)
G-2	143.3±63.5 (2451)	142.9±69.4 (552)	113.6±36.0 (640)	136.4±56.5 (637)	181.1±68.3 (622)
G-3	146.7±73.2 (2430)	149.2±80.5 (551)	111.1±38.9 (640)	136.7±61.8 (635)	192.5±80.7 (604)
G-4	104.4±47.5 (2451)	108.5±53.7 (552)	74.7±20.2 (640)	95.5±33.2 (637)	140.3±50.1 (622)
G-5	144.7±66.2 (2425)	157.6±76.1 (552)	113.5±35.0 (640)	127.3±47.4 (626)	183.7±74.9 (607)
G-6	125.1±62.9 (2414)	140.4±70.3 (551)	98.5±34.4 (640)	116.0±56.3 (636)	149.4±72.6 (587)
G-7	96.6±39.1 (2444)	109.6±45.8 (552)	76.3±21.9 (640)	88.8±30.9 (637)	114.3±41.8 (615)
G-8	124.8±55.6 (2432)	132.0±55.3 (551)	101.8±34.3 (639)	123.1±57.1 (636)	144.3±63.1 (606)
Northern Zone[c]	**117.9±41.0** (2451)	**127.9±44.4** (552)	**90.3±17.9** (640)	**107.9±32.8** (637)	**147.8±39.9** (622)
G-9	98.9±47.6 (2451)	110.4±51.1 (552)	78.0±28.4 (640)	99.3±46.7 (637)	109.9±53.6 (622)
G-10	116.6±55.1 (2449)	118.4±50.5 (552)	86.6±29.9 (640)	123.4±53.2 (637)	139.1±66.5 (620)
G-11	118.0±46.8 (2451)	128.0±48.9 (552)	98.3±33.7 (640)	107.9±41.4 (637)	139.7±50.3 (622)
Middle Zone	**104.1±43.0** (2451)	**112.8±42.9** (552)	**81.5±22.7** (640)	**104.3±41.0** (637)	**119.5±50.7** (622)
G-12	74.9±28.1 (2106)	81.4±29.2 (498)	61.5±21.4 (520)	73.6±27.3 (58 1)	83.7±28.6 (506)
G-13	49.9±14.5 (2451)	48.8±12.7 (552)	40.9±10.5 (640)	53.9±14.0 (637)	55.9±15.4 (622)
G-14	63.4±24.0 (2451)	66.5±24.0 (552)	47.5±13.0 (640)	66.7±22.0 (637)	73.4±26.8 (622)
Southern Zone	**58.2±17.7** (2451)	**59.8±16.6** (552)	**45.4±9.5** (640)	**61.6±16.3** (637)	**66.5±19.4** (622)
Kelamayi	57.5±39.9 (990)	53.5±25.0 (183)	57.8±17.5 (273)	68.7±64.9 (273)	48.4±25.8 (261)
Urumchi	156.2±134.5 (2073)	123.9±102.1 (428)	73.9±40.9 (640)	141.8±101.8 (575)	329.9±137.8 (430)
Lhasa	64.7±37.1 (2451)	78.4±36.2 (552)	41.5±19.6 (640)	59.5±28.7 (637)	81.9±44.6 (622)

[a] Concentrations in micrograms per cubic meter calculated from daily geometric mean PM_{10} for the group/zone.
[b] Here, *n*, number of daily geometric mean PM_{10} concentrations for the group/zone.
[c] The three latitudinal zones are same as those illustrated in Fig. 2.

ACPD
9, 23141–23185, 2009

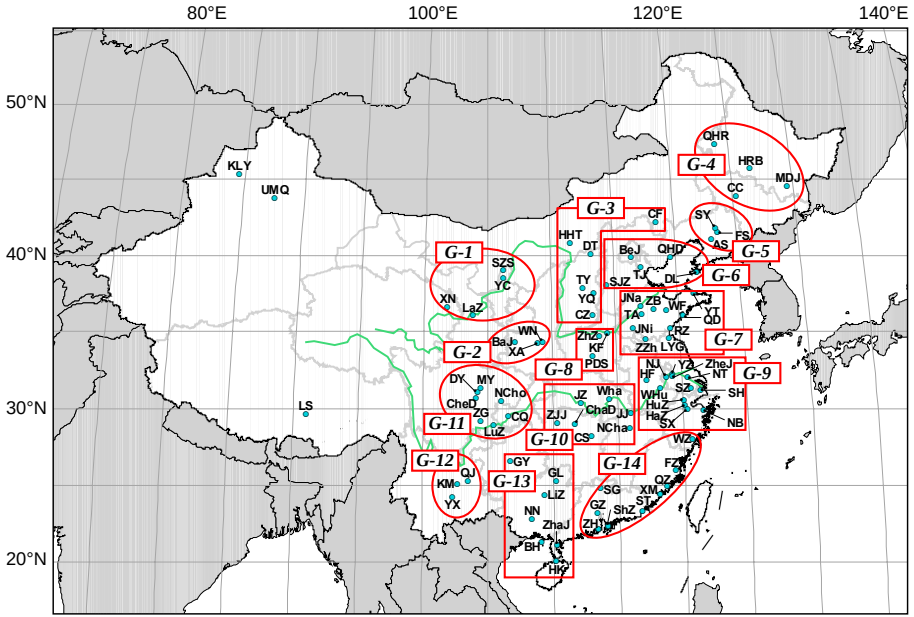

Fig. 1. Locations of the 86 cities in China. Full name of these cities are listed in Table 1. Red frame labeled with G-1 through to G-14 included the cities attributed to the specific group as in Table 1.

ACPD
9, 23141–23185, 2009

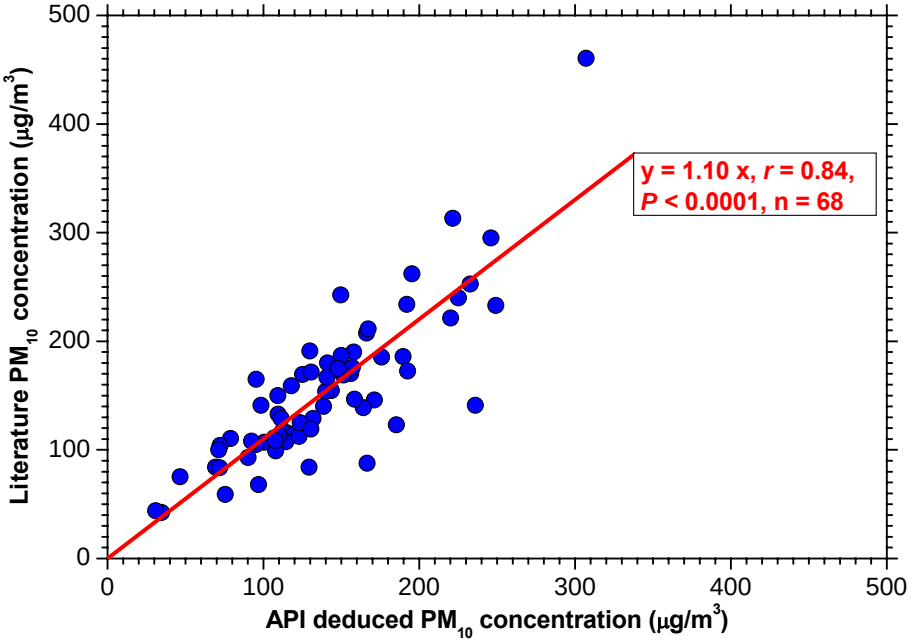

Fig. 2. Linear correlation between the API deduced PM_{10} concentration and the literatures reported PM_{10} concentration. The data used in this analysis are adapted from those shown in the supplementary material 1 (http://www.atmos-chem-phys-discuss.net/9/23141/2009/acpd-9-23141-2009-supplement.zip) – Validation of the API deduced PM_{10} data.

ACPD
9, 23141–23185, 2009

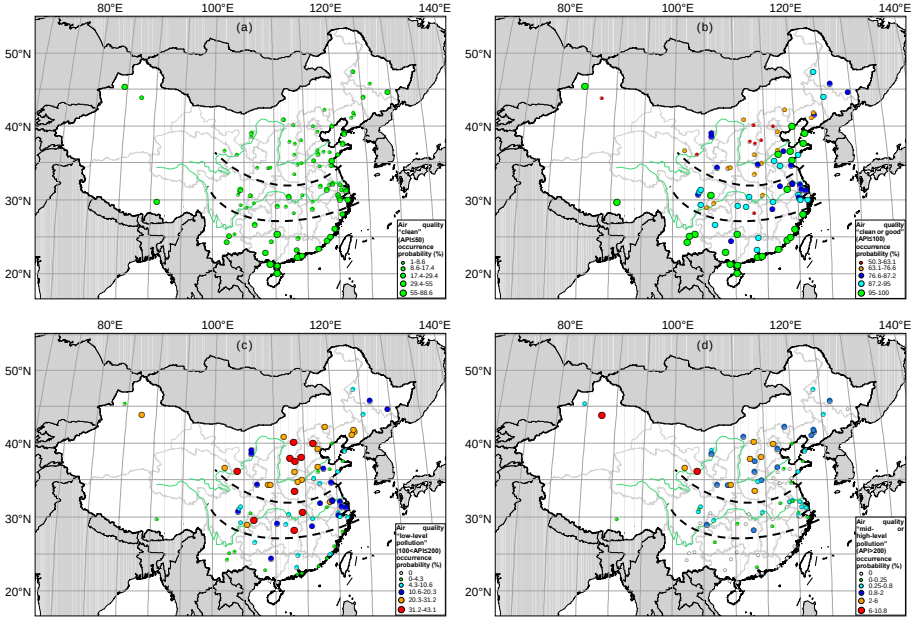

Fig. 3. Spatial distribution of the occurrence probability of the days with air quality classification as **(a)** "clean (API≤50)", **(b)** "clean or good (API≤100)", **(c)** "low-level pollution (100<API≤200)" and **(d)** "mid- or high-level pollution (API>200)" for the 86 cities. The 83 cities in middle-eastern China were further partitioned into three latitudinal zones between the black dash lines, these included the northern zone (north of 33° N latitude, including 38 cities, i.e. G-1, G-2, G-3, G-4, G-5, G-6, G-7 and G-8) extended westward to the northeastern margin of the Tibetan Plateau, northward to the boundary between China with Mongolia and Russia, eastward to the Japan sea, the Bohai sea and the Yellow sea, and southward with boundary line of the Qinlin Mountain – the Huaihe River between the middle zone; the middle zone (between 28° N to 33° N latitude, including 26 cities, i.e. G-9, G-10 and G-11) extended westward to the eastern margin of the Tibetan Plateau, eastward to the Yellow sea and the East China sea and southward with boundary line of the Dalou Mountain on the northeastern margin of the Yunnan-Guizhou Plateau – the Jiangnan Hill – the Wuyi Mountain; and the southern zone (south of 28° N latitude, including 19 cities, i.e. G-12, G-13 and G-14) extended westward to the southeastern margin of the Tibetan Plateau, eastward to the East China sea and Taiwan Island, southward to the South China sea. Kelamayi, Urumchi and Lhasa in western China were not included in these three zones.

ACPD
9, 23141–23185, 2009

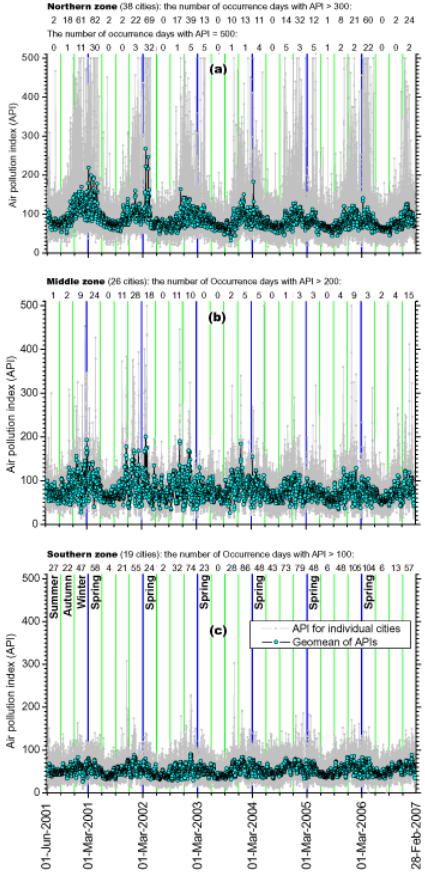

Fig. 4. Variation of the daily air pollution indexes (APIs) for the northern **(a)**, middle **(b)** and southern **(c)** latitudinal zones. Light gray dots linked with light gray straight solid lines denotes daily APIs for the individual cities, while cyan dots linked with black straight solid lines donates daily geometric mean APIs for the three latitudinal zones. The numbers of occurrence days with high APIs for the cities in the three latitudinal zones are also presented at the top of (a), (b) and (c).

ACPD
9, 23141–23185, 2009

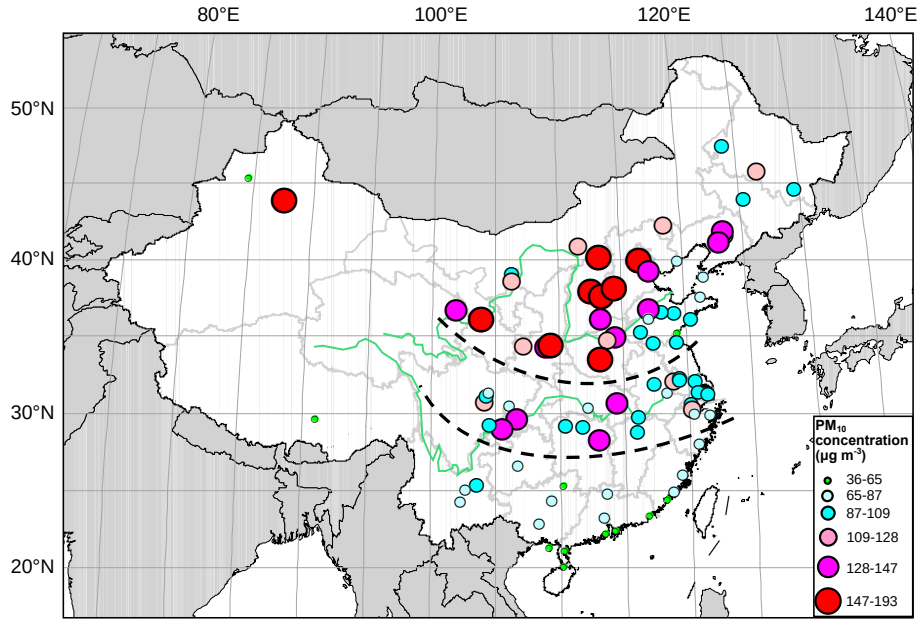

Fig. 5. Spatial distribution of the multi-year (2000–2006) average PM_{10} concentrations for the 86 individual cities.

ACPD
9, 23141–23185, 2009

CC BY

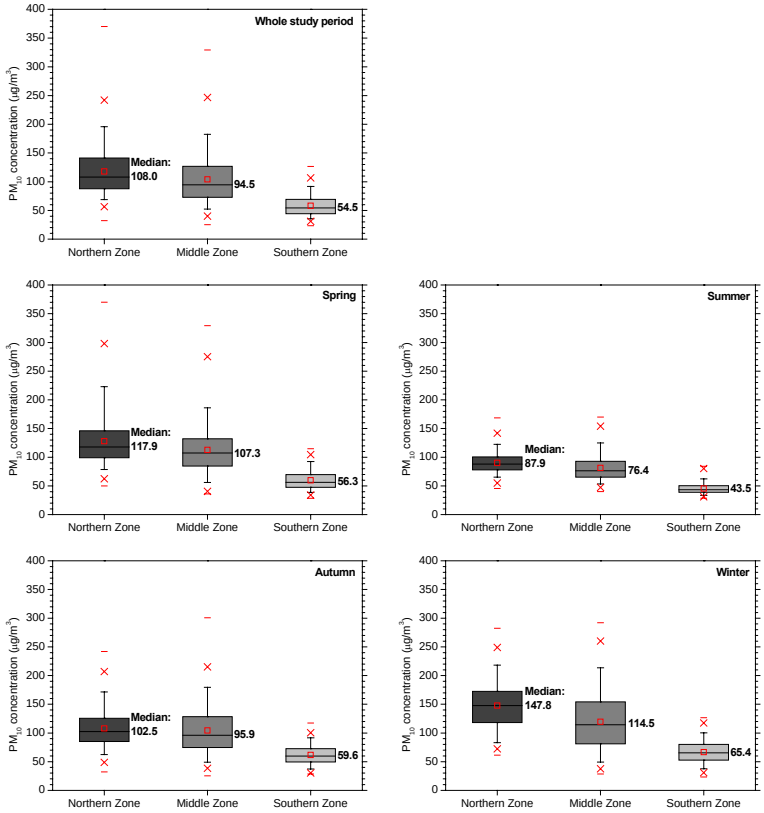

Fig. 6. Comparison of PM_{10} levels and variations for the three latitudinal zones in different seasons, the box-and-stem plots depict the minimum, the 1th, 5th, 25th, 50th (median), 75th, 95th, 99th percentile and the maximum for the PM_{10} concentration, the little red square in the box depicts the arithmetic mean PM_{10} concentration, the median PM_{10} concentrations for the three latitudinal zones are also presented.

ACPD
9, 23141–23185, 2009

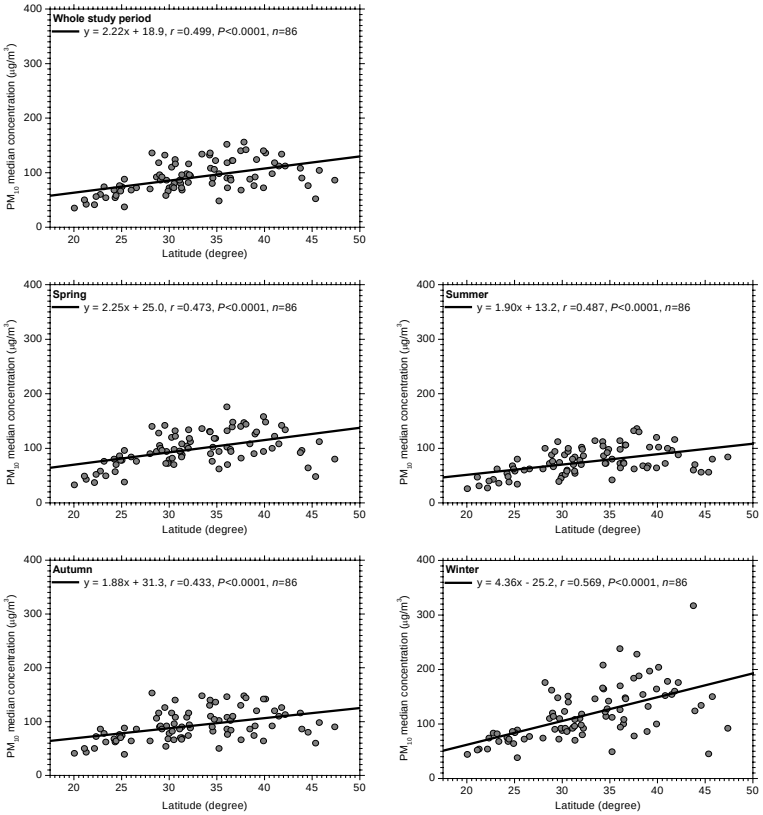

Fig. 7. Latitudinal PM_{10} gradient denotes by linear fitting of PM_{10} median concentration with latitude for the 86 cities in different seasons. The latitudinal gradient (north to south decrease) of PM_{10} levels was illustrated by significant linear fittings ($p<0.0001$ significance) of PM_{10} median concentration with latitude of the cities. Note that the north to south decreasing trends of PM_{10} levels were not strictly linear; the points illustrated PM_{10} median concentrations for the cities tended to be low at both the lower and upper ends of the latitude range.

ACPD
9, 23141–23185, 2009

CC BY

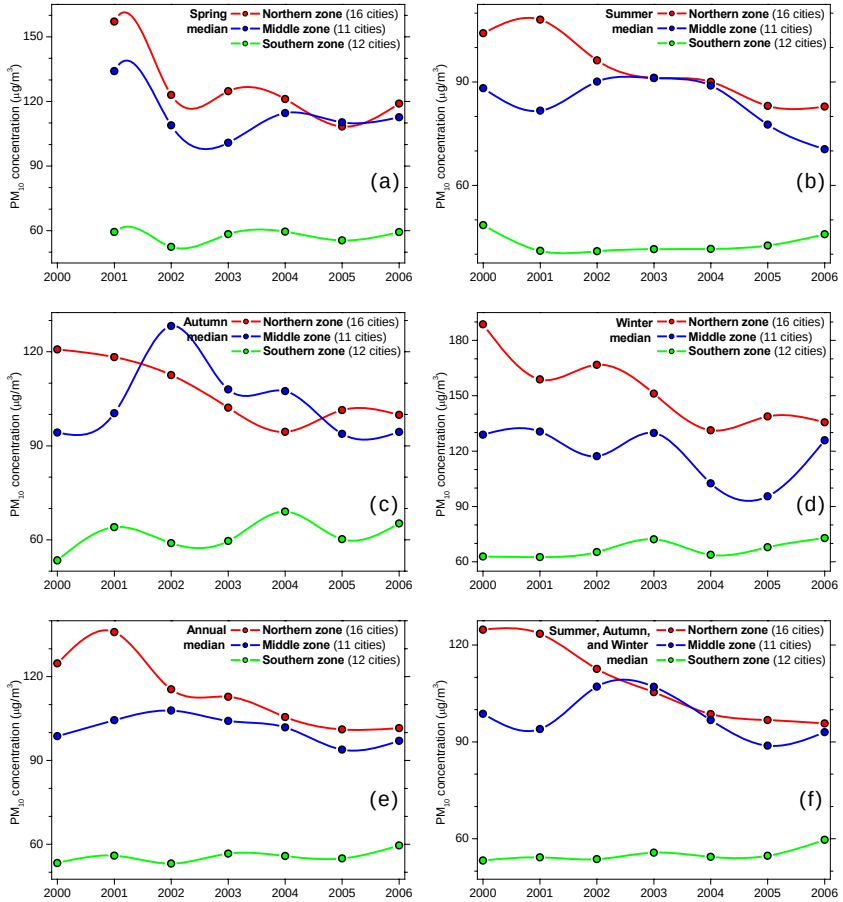

Fig. 8. Interannual variation of the **(a)** spring, **(b)** summer, **(c)** autumn, **(d)** winter, **(e)** annual, and **(f)** summer, autumn and winter median PM_{10} concentrations for the three latitudinal zones during 2000 to 2006.

CC BY